Stimulation of immunity-linked genes by membrane disruption is linked to Golgi function and the ARF-1 GTPase

Christofer M. Welsh[1], Lorissa J. Smulan[2], Matthew J. Fanelli[1], Dominique S. Lui[1], and Amy K. Walker[1]

[1]Program in Molecular Medicine, UMASS Medical School, Worcester, MA

[2]Department of Medicine, UMASS Medical School, Worcester, MA

Contact: amy.walker@umassmed.edu

Summary

Immune-linked genes (ILGs) are activated in response to pathogens but can also be activated by lipid imbalance. Why pathogen attack and metabolic changes both impact ILG activation is unclear. Organelles in the secretory pathway have distinct protein and lipid components and genetically separable stress programs. These stress pathways activate restorative transcriptional programs when lipid ratios become unbalanced or during dysregulated protein folding and trafficking. We find that ILGs are specifically activated when membrane phosphatidylcholine ratios change in the secretory pathway. Consistent with this result, disruption of Golgi function after RNAi targeting the ADP-ribosylation factor ARF-1 also activates ILG expression. Since increased protein secretion is altered by metabolic changes and pathogen responses, our data argue that ILG upregulation is a conserved, coordinated response to changes in trafficking resulting from intrinsic cues (lipid changes) or extrinsic stimulation (during the immune response). These findings uncover important and previously unexplored links between metabolism and the stress response.

33 **Introduction**

34 Cellular stress responses both react to extrinsic insults by upregulating genes that
35 defend the cell. Stress responses also restore organelle function in response to intrinsic
36 changes. Several of these intrinsic stress response pathways are also linked to
37 metabolic processes. For example, overnutrition can lead to metabolic changes that
38 induce cellular stress through an increase in reactive oxygen species (Wellen and
39 Thompson, 2010). Several signaling pathways play a dual role, functioning as
40 coordinators of nutrient responses as well as stress responses. For example, the
41 nutritional sensor mTORC1 can influence stress-responsive transcription (Aramburu et
42 al., 2014). In addition, insulin signaling pathways are strongly linked to stress. For
43 example, mutations in *daf-2*, the *Caenorhabditis elegans* insulin receptor/insulin-like
44 growth factor ortholog, produce highly stress-resistant animals (Son et al., 2019).
45 Finally, changes in ER lipids have a profound effect on stress pathways (Gianfrancesco
46 et al., 2018; Halbleib et al., 2017; Koh et al., 2018). Specialized ER sensors detect both
47 the accumulation of unfolded proteins and overload of the secretory pathway. These
48 sensors then initiate gene expression programs that reduce protein load or increase
49 lipid production (reviewed in: Hotamisligil and Davis, 2016; Radanović et al., 2018).
50

51 While stress responses and metabolism are clearly intertwined, the biological
52 advantages of linking these processes are less clear. For example, in a previous study,
53 we found that RNAi-mediated knockdown of two different lipid synthesis modulators,
54 *sams-1* and *sbp-1*, caused upregulation of pathogen-response genes in *C. elegans*
55 (Ding et al., 2015). One of these lipid modulators, *sams-1/MAT1A,* encodes an S-

56 adenosylmethionine synthase important for phosphatidylcholine (PC) production
57 (Walker et al., 2011). The Troemel lab also identified *sams-1* as a regulator of the
58 infection response gene *irg-1* in an RNAi screen (Dunbar et al., 2012). The other lipid
59 modulator identified in our previous screen, *sbp-1/SREBPF1,* codes for a master
60 transcriptional regulator of lipid synthesis genes (Horton et al., 2002). Reduction of *sbp-*
61 *1/SREBPF1* causes a decrease in total lipid stores (McKay et al., 2003). Notably,
62 mammalian SREBPF1 knockdown also results in the enrichment of immunity-linked
63 gene expression in human cells (Wu and Näär, 2019). Recent studies from other labs
64 have found that ILGs are upregulated after mutation or RNAi of genes affecting PC
65 synthesis. ILG activation was seen upon disruption of *pmt-2* (Ho et al., 2020) or *lpin-1* in
66 the presence of excessive glucose (Jung et al., 2020). These immune-linked genes
67 were also upregulated in *skn-1* mutants, a transcriptional regulator of the stress
68 response and metabolic genes (Nhan et al., 2019). In addition, dietary restriction
69 results in the upregulation of similar gene sets (Wu et al., 2019). These results together
70 suggest that multiple types of lipid imbalance seem to impact immunity-linked gene
71 expression and that these links may be conserved across species, as indicated by
72 results in human cells cited above .
73
74 Exposure of *C. elegans* to bacterial pathogens stimulates the expression of a diverse
75 set of genes, including antimicrobial peptides, enzymes for detoxifying xenobiotics, and
76 neuromodulatory peptides to coordinate inter-organ defenses (Engelmann et al., 2011;
77 Fletcher et al., 2019; Mallo et al., 2002; Troemel et al., 2006). However, many of the
78 genes upregulated in response to either bacteria or fungi do not fall into these clearly

defensive pathways (Estes et al., 2010) or have clear functional roles and are instead defined by pathogen-responsive expression. In order to understand the relationship between ILG regulation and changes in lipid levels, we compared lipidomics from *sams-1* and *sbp-1* animals with results from a targeted RNAi screen for activation of the immunity-linked reporter, p*sysm-1::GFP* (Shivers et al., 2009). We found that *sams-1 and sbp-1* knockdown animals both had broad changes in their lipidome. However, fractionated *sbp-1* extracts showed low PC in the ER/Golgi fraction, as we previously found in *sams-1* animals (Smulan et al., 2016). Our targeted RNAi screen argues that synthesis of two lipid classes, PC and sphingomyelin (SM), increase p*sysm-1::GFP* expression. In addition, RNAi of Golgi/ER transport regulators, including the GTPase *arf-1/ARF1,* activated the immunity-linked reporter. Notably, some ILGs were also upregulated after *arf-1*/ARF1 RNAi, suggesting that disrupting Golgi function regulates immunity-linked genes. Finally, we find that RNAi of one ILG, *hpo-6*, disrupts the trafficking of two secreted proteins. Taken together, our results suggest that some ILGs act to balance the increased secretory load in pathogen-stimulated cells. While immune function is critical for host defenses, immune activation in non-pathogenic conditions, such as in metabolic disease, may have deleterious effects (Zmora et al., 2017). Thus, our studies provide critical links between shifts in lipid metabolism and stimulation of immunity-linked gene expression.

99 ## Results

100 ***Gene set enrichment shows upregulation of pathogen-response genes in multiple***
101 ***models of membrane dysfunction***

102 Levels of lipids within membranes are tightly monitored, and imbalances may induce
103 cellular stress pathways that regulate genes to restore lipid ratios (Hotamisligil and
104 Davis, 2016). We previously found that *sams-1*, *lpin-1,* and *sbp-1* are part of a
105 feedback loop that responds to shifts in membrane PC levels and activates immunity-
106 linked genes (Fig. 1A; Smulan et al., 2016; Walker et al., 2011). In order to test why
107 immunity-linked genes are activated after disruption of lipid-synthesis regulators we first
108 conducted a bioinformatics analysis using our recently developed *C. elegans* specific
109 gene ontology tool, WormCat 2.0. This computational analysis allows combinatorial
110 graphing of gene enrichment scores based on detailed annotation of all *C. elegans*
111 genes (Higgins et al., 2021; Holdorf et al., 2019). This tool uses a nested annotation
112 strategy (Category1/Category2/Category3) to provide broader or more detailed
113 information on genome-wide datasets. In order to better characterize these ILGs, we
114 used WormCat to directly compare genes upregulated in the *sams-1, sbp-1,* and *lpin-1*
115 mutants (**Fig1A**). The Lee lab generously shared data of genes that are upregulated
116 when *lpin-1* is knocked down in the absence of the stress-triggering glucose (Jung et
117 al., 2020) **Table S1**). WormCat analysis indicates that all three knockdowns result in
118 enrichment in the broad Category1(Cat1) STRESS RESPONSE category, and more
119 specifically in Pathogen at the Cat2 level, similar to results from GO analysis (**Fig1A-**
120 **C)**. Notably, the strongest enrichments at the Cat3 level were in STRESS RESPONSE:
121 Pathogen: *other*. This category contains genes that increase upon pathogen exposure

122 in *C. elegans* but do not have defined functions as antimicrobial peptides or within
123 pathogen-stimulated signaling pathways such as MAPK signaling (Higgins et al., 2021;
124 Holdorf et al., 2019). This class of genes is not explicitly defined by a traditional GO
125 analysis. We also noted that the landscape of upregulated genes was complex, with
126 STRESS RESPONSE: Detoxification enrichment scores increasing in both *sams-1* and
127 *lpin-1* but not *sbp-1* (**Fig1B**). In addition, METABOLISM: Lipid was increased after
128 *sams-1* and *lpin-1* RNAi (**Fig1B**). These data are consistent with our previous studies
129 showing that SBP-1 transcriptional targets are upregulated in these animals (Walker et
130 al., 2011), as are immunity-linked categories after SREBP-1 knockdown in human
131 melanoma cell lines (Wu and Näär, 2019). Finally, WormCat analysis of microarray
132 data from the Thibault lab (Koh et al., 2018) finds that STRESS RESPONSE: Pathogen
133 is increased after knockdown of *pmt-2*, a methyltransferase essential in SAM-dependent
134 PC production (**FigS1A**). Thus, genes linked to immunity are upregulated across a
135 diverse set of lipid synthesis modulators in *C. elegans* and mammalian cells.
136
137 SBP-1/SREBP1 is a basic helix-loop-helix transcription factor required to express a
138 suite of lipid metabolic genes, including *fat-7* in *C. elegans* and its ortholog SCD1 in
139 mammals (HORTON et al., 2002; McKay et al., 2003). It is also necessary for the
140 upregulation of *fat-7* in lipid-replete *sams-1(lof)* animals ((Walker et al., 2011), and
141 **Fig1D**). Since SBP-1 upregulates lipid synthesis genes, we tested the possibility that it
142 directly functions in ILG upregulation by using *sams-1(RNAi)* to increase the expression
143 of multiple SBP-1 target genes (Walker et al., 2011). Whereas *fat-7* depends on *sbp-1*
144 in both the control and *sams-1(RNAi)* background, *hpo-6* is expressed at high levels in

145 both *sbp-1(RNAi)* and *sams-1(lof); sbp-1(RNAi)* animals (**Fig1D**). This suggests that
146 the effects of SBP-1 on ILG upregulation are indirectly related to its function as a
147 transcriptional regulator.
148
149 Many pathogen-responsive genes in *C. elegans* act downstream of signals from the
150 p38/MAPK14 kinase PMK-1 (Troemel et al., 2006). In previous studies in *C .elegans*,
151 we found that low PC in *sams-1(lof)* animals leads to constitutive phosphorylation of
152 PMK-1 and that ILG induction was dependent on both PC and *pmk-1* (Ding et al., 2015).
153 In order to confirm this effect in mammalian cells, we used siRNA to knock down the
154 rate-limiting enzyme for PC production, *PCYT1,* in human hepatoma cells (**FigS1B**). We
155 found that p38/MAPK14 phosphorylation is induced to levels similar to
156 lipopolysaccharide (LPS). In *C. elegans*, knockdown of *sbp-1* also induces PMK-1
157 phosphorylation (**FigS1C**). Taken together, the results suggest that upregulation of
158 ILGs in response to lipid perturbations may share regulatory link to pathogen-stimulated
159 pathways.
160
161 ***Loss of sbp-1 decreases PC levels in ER/Golgi extracts***
162 Immunity-linked gene expression and PMK-1 phosphorylation both occur after reduction
163 in *sams-1* and *sbp-1*, although these genes act at different points in lipid synthesis
164 regulation. Next, we sought to identify any shared signatures in the total lipidomes of
165 these mutants by LC/MS. Because animals were lysed directly into lipid extraction
166 buffer, levels were normalized to total lipid as in (Smulan et al., 2016). The entire
167 lipidome was broadly altered in both cases, with 27% of lipid species showing significant

168 changes in *sams-1(RNAi)* animals and 30% after *sbp-1(RNAi)* (**Fig2A, B; Table S2**).
169 We next examined lipid levels at the class and species level. As in our previous studies
170 (Cell 2011), *sams-1* animals showed lower PC and higher TAG (**Fig2C**), and we also
171 noted lower phosphatidylserine (PS) and SM levels in comparison to other lipid classes
172 (**Fig2C, FigS1C**). TAG was lower after *sbp-1* RNAi, as expected from previous studies
173 (Yang et al., 2006). We also found that while reductions in PC did not reach
174 significance, PE increased, and Cer levels dropped (**Fig2C, D**). In short, *sbp-1* RNAi
175 induces broad changes in the lipidome across multiple classes of lipids.
176
177 The properties of lipid classes can be altered when distributions of acyl chains change
178 significantly. We find that there are significant differences in the populations of species
179 within phospholipids (PC, phosphatidylethanolamine (PE), lyso-
180 phosphatidylethanolamine (LPE), and phosphatidylglycerol (PG), triglycerides (TAG),
181 diacylglycerides (DG), and sphingomyelins (SM) after *sams-1(RNAi)*. Changes in
182 species distribution in lipid classes after *sbp-1* RNAi were limited to TAG, lyso-
183 phosphatidylcholine (LPC), and ceramides (Cer) in agreement with previous studies
184 showing lower TAGs in *sbp-1(RNAi)* animals. We asked if *sams-1* and *sbp-1* RNAi
185 caused similar shifts in animals and found overlapping changes in 180 shared lipid
186 species (**TableS2**). 57 of these species were decreased in both, 17 increased in both,
187 and 102 lipid species changed in opposite directions out of 1405 total lipid species
188 detected. Lipid species diverged most strongly within the TG class, with increases in
189 *sams-1(RNAi)* animals and decreases after *sbp-1* RNAi (**TableS2**). This agreed with
190 total class levels. For lipid species that increased in both animals, PE species were the

191 highest, with 15 changing at significant levels. 74 PC species changed in both *sams-1*
192 and *sbp-1* animals, with 35 decreasing in both (**TableS2**). Finally, three SM species
193 decreased in both animals. Thus, while *sams-1* or *sbp-1* knockdown each lead to broad
194 changes in the total lipidome, relatively few overlapping species changed in both
195 instances. Of those, PC species were the best represented among lipid species that
196 decreased upon knockdown of either *sams-1* or *sbp-1* in animals.
197
198 The total lipidome contains multiple organelles, including the plasma membrane,
199 mitochondria, nuclear membrane, and Golgi/ER. However, lipid ratios in specific
200 organelles may be reflective of particular functions; for example, we previously found
201 that PC ratios in ER/Golgi fractions were associated with activation of SBP-1 in *sams-1*
202 and *lpin-1* animals (Smulan et al., 2016). Therefore, we performed LC/MS lipidomics on
203 microsomes from *sbp-1(RNAi)* animals. Because the lipidomics was performed on
204 fractionated animals, we used total protein for normalization. We found a broader
205 fraction of the ER/Golgi lipidome was affected after *sbp-1(RNAi)* than in the total lipid
206 samples. Nearly 40% of lipid species were altered in these fractions (**Fig2E; Table S2**),
207 with significant changes in species across most classes (**FigS1C**). Similar to the
208 unfractionated extracts, levels of TAG and Cer decreased in the ER/Golgi (**Fig2F**).
209 Notably, significant ER/Golgi-specific decreases occurred in PC and DG (**Fig2F, G;**
210 **FigS1D**). This demonstrates that *sbp-1(RNAi)* has distinct effects on the ER/Golgi
211 membranes and shows decreases in PC levels at the sub-compartment level, similar to
212 *sams-1* RNAi.
213

214 ***Targeted RNAi Screen Reveals roles for Ceramide/Sphingomyelin synthesis and***
215 ***COP I transport in immune gene expression***
216 Low PC levels are associated with ILG expression in *sams-1* (Ding et al., 2015) and
217 *pmt-2(RNAi)* animals (Koh et al., 2018). The low PC in the ER/Golgi compartment of
218 both *sams-1* (Smulan et al., 2016) and *sbp-1* RNAi animals suggests this could be a
219 shared signature linked to ILG upregulation. To understand how these lipids might act,
220 we next sought to identify genes important for ILG expression. We screened for
221 upregulation of an immune reporter, p*sysm-1*::GFP (Shivers et al., 2009), with an RNAi
222 sub-library that targets genes involved in complex lipid metabolism, lipid signaling and
223 selected ER/Golgi transport regulators. We previously used a lipid-function RNAi sub-
224 library to identify low-PC regulators of SBP-1/SREBP-1 (Smulan et al., 2016). Notably,
225 we constructed RNAi clones for genes not represented in the Arhinger or Orfeome RNAi
226 libraries. The resulting library includes all predicted phospholipases and enzymes for
227 synthesis of complex lipids (Smulan et al., 2016). For the current screen, we expanded
228 the sub-library to include more genes involved in ceramide/sphingomyelin synthesis and
229 confirmed all clone identities by sequencing. Thus, this library has a broader
230 representation of genes linked to complex lipid synthesis than the commercially
231 available RNAi libraries. p*sysm-1*::GFP is strongly induced by *sbp-1(RNAi)* (**Fig3A**) and
232 has been used by multiple labs as a robust marker for immune gene induction (Jeong et
233 al., 2017; Pender and Horvitz, 2018; Wu et al., 2019).
234
235 In order to identify genes in lipid synthesis important for ILG upregualion, we screened
236 this library in quadruplicate in p*sysm-1*::GFP animals and identified a list of 20

237 candidates for retesting (**Fig3B; Table S3**). Retesting to identify the strongest
238 candidates occurred in 3 stages: visual rescreening (4X), imaging of candidates from
239 the rescreen, and qRT-PCR to assess changes in GFP expression. We also included
240 the *sbp-1* target genes *fat-5*, *fat-6,* and *fat-7* (McKay et al., 2003; Yang et al., 2006) in
241 the visual retesting. These genes are orthologs of mammalian Stearoyl CoA
242 desaturases (SCDs) (Watts and Browse, 2002) and can change membrane fluidity
243 (Bodhicharla et al., 2018; Ruiz et al., 2018) or induce lipid bilayer stress by changing
244 ratios of saturated/unsaturated acyl chains within lipid classes (Ho et al., 2018, 2020;
245 Koh et al., 2018).
246
247 Candidates from the targeted screen fell into two major groups. First, enzymes linked to
248 PC and SM synthesis were found (**Fig3C-G; FigS3A, B; TableS3**). This included two
249 isoforms of the rate-limiting enzyme for PC production, *pcyt-1,* and *sptl-1*, which initiates
250 the first committed step in sphingolipid synthesis. Thus, our genetic data supports the
251 notion that changes in PC or SMs are a shared signature linked to ILG activation in
252 *sams-1* and *sbp-1* RNAi animals. Notably, *fat-5, -6,* or *fat-7* RNAi, which would change
253 acyl chains saturation within each lipid class, had modest effects on the p*sysm-1*::GFP
254 immune reporter (**Fig3H, FigS3A, B; Table S3**), suggesting changes in membrane
255 fluidity downstream of these enzymes is not a major contributor to the immunity-linked
256 gene upregulation.
257
258 Second, genes involved in Golgi/ER trafficking activated the reporter in both strains
259 (**Fig3C, D; Fig43A, B; TableS3**). Golgi/ER trafficking genes included four genes

260 forming the COPI complex (which also caused developmental delays) and ARF1
261 guanine activating factor (*agef-1*). The ARF-1 GTPase, a key regulator of these factors,
262 was a false negative in the original screen, but strongly activated the reporter in the
263 rescreening. (**Fig3I**; **Table S3**). The coatomer proteins work in a complex (Spang, 2002)
264 and are required for viability (Fraser et al., 2000). Therefore, we chose one candidate,
265 *copa-1,* and performed RNAi with diluted bacteria, allowing animals to develop fully.
266 We found that the immune activation reporter was strongly expressed in the *copa-1*
267 knockdown (**Fig3I**). Stimulation of the reporter after the loss of multiple parts of the
268 COP I machinery and its key regulator *arf-1* strongly argues that ER/Golgi dynamics
269 signal to induce immunity-linked genes.
270
271 The p*sysm-1*::GFP reporter represents a single gene in the immune response program.
272 To more broadly survey ILGs in our screen validation, we used qRT-PCR with primers
273 specific to the endogenous *sysm-1* gene, *irg-1, irg-2,* and *hpo-6*, and found robust
274 activation of each of our candidate reporters after knockdown of *arf-1* or *copa-1*, but
275 more modest effects with the SM genes or SCDs (**FigS4C-G)**. Integration of results
276 from this targeted RNAi screen with our lipidomics studies shows overlap in two main
277 areas, PC and SM synthesis, which are themselves connected. We previously linked
278 changes in PC levels in *sams-1* microsomes to the inactivation of ARF-1, which drove
279 proteolytic processing of SBP-1/SREBP-1 (Smulan et al., 2016). These results suggest
280 that blocking ARF-1 function could also be linked to ILG activation.
281
282 ***Disruption of ER/Golgi activates immunity-linked genes***

283 The upregulation of *sysm-1* and other immune genes after *arf-1* RNAi prompted us to
284 examine genome-wide changes in the transcriptome that could occur in response to the
285 loss of ARF-1 function. Using RNA-seq, we found that 705 genes were significantly
286 upregulated after *arf-1* RNAi (**Fig4A, FigS3A; Table S4**) and that 40% of these genes
287 were also upregulated in *sams-1* or *sbp-1* RNAi animals (**FigS4A**). Downregulated
288 genes in *sams-1, sbp-1,* or *arf-1* animals had low levels of overlap (**FigS4B**). WormCat
289 gene set enrichment shows that STRESS RESPONSE: Pathogen: *Other* gene sets are
290 significantly upregulated in *arf-1(RNAi)* animals as they are after *sbp-1, sams-1,* or *lpin-*
291 *1* RNAi (**Fig4B**). Next, we examined WormCat enrichment within the genes that were
292 shared between these three RNAi sets and found that shared genes retained strong
293 enrichment for STRESS RESPONSE: Pathogen (**FigS4C-D**). Thus, *arf-1* GTPase
294 knockdown causes similar or overlapping effects in immune gene expression to those
295 seen after broad lipid disruption by *sbp-1* RNAi. Cycling of the ARF1 GTPase requires
296 interaction with the Golgi membrane (Spang, 2002). In order to study the localization of
297 ARF-1, we obtained a strain where endogenous ARF-1 is C-terminally tagged by
298 CRISPR. Next, we asked if ARF-1 localization was altered in *sbp-1(RNAi)* animals by
299 examining expression in the ARF-1::RFP animals. In intestinal cells, ARF-1::RFP
300 formed a punctate pattern (**Fig4C**) similar to that of the Golgi ministacks characteristic
301 of *C. elegans* cells (Broekhuis et al., 2013) (See also **Fig4D**). Strikingly, ARF-1::RFP
302 appeared to form larger, more irregular punctae in *sbp-1(RNAi)* animals as well as
303 having additional diffuse localization, similar to patterns seen with RNAi of the coatomer
304 protein COPA-1 (**Fig4C**). This suggests that ARF-1 functions at the Golgi are altered in
305 *sbp-1(RNAi)* animals.

306

307 Loss of human ARF1 or blocking ARF1 cycling with the fungal toxin BrefeldinA disrupts
308 Golgi integrity (Klausner et al., 1992). In addition, our previous studies found that
309 lowering PC levels through RNAi of *sams-1* or knockdown of *PCYT1* (the rate-limiting
310 enzyme for PC production) in mammalian cells blocked ARF1 GTPase activity and
311 disrupted Golgi structure (Smulan et al., 2016; Walker et al., 2011). Because PC levels
312 in *sbp-1(RNAi)* ER/Golgi fractions decreased (**Fig2C**) and ARF-1::RFP was
313 mislocalized, we next examined Golgi structure in *sbp-1(RNAi)* animals using a reporter,
314 MANS::GFP, driven by an intestinal reporter (Chen et al., 2006). MANS::GFP is a
315 fusion of *aman-2* (alpha-mannosidase, a conserved Golgi specific protein) and marks
316 the mini-Golgi stacks characteristic of *C. elegans* (Rolls et al., 2002). Consistent with
317 previous studies (Ackema et al., 2013; Sato et al., 2006), knockdown of *arf-1*
318 dramatically shifts the Golgi puncta to diffuse localization across the cytoplasm (**Fig4D**).
319 *copa-1* RNAi also diminished Golgi stacks along with altering ARF-1::RFP localization
320 (**Fig4C, D**). *sbp-1* knockdown affects Golgi structure, but results in a different pattern
321 (**Fig4E**). Golgi stacks are more numerous and smaller with increases in diffuse
322 cytoplasmic localization (**Fig4E**). Notably, *sptl-1(RNAi)* did not noticeably alter Golgi
323 marked by MANS::GFP and ARF-1::RFP puncta were visible, suggesting that *sptl-1*
324 knockdown may mediate effects on immune genes through and SM pathways through
325 different cellular membranes. Taken together, we find that ARF-1 activity (Smulan et
326 al., 2016) and localization (this study) can be affected by *sams-1* or *sbp-1* RNAi and that
327 targeting *arf-1* or the coatomer components can activate ILGs. Thus, blocking or
328 limiting ARF-1 function at the Golgi may be part of the signal to activate these genes.

329

330 ***Immunity-linked gene upregulation in models of trafficking dysfunction***

331 The Golgi apparatus accepts proteins from the ER that are destined for secretion,
332 processing them by glycosylation before secretory vesicles are loaded (Boncompain
333 and Weigel, 2018). Stimulation of the innate immune system may significantly impact
334 trafficking load, as antimicrobial peptides are shuttled through the membrane trafficking
335 system (Taguchi and Mukai, 2019). Indeed activation of the ER stress response has
336 been noted in multiple systems when large numbers of proteins need to be produced
337 and secreted (Gardner et al., 2013). Interestingly, previous data suggest that induction
338 of membrane stress may also be a sensor of infection (Lamitina and Chevet, 2012).
339 Based on work by the Ewbank lab, they also suggested that some pathogen-response
340 genes act to support the trafficking of antimicrobial peptides (AMPs) (Couillault et al.,
341 2012; Lamitina and Chevet, 2012). We noted that the immunity-linked genes
342 upregulated at low PC are largely outside of the antimicrobial categories and are
343 comprised of gene sets defined by their shared expression upon pathogen exposure
344 rather than function (Estes et al., 2010; Holdorf et al., 2019). We hypothesized that
345 some of these genes might be responding to direct stress on the trafficking system.

346

347 To explore this idea, we turned to two commonly used systems for studying trafficking in
348 *C. elegans*, visualization of VIT-2::GFP (Grant and Sato, 2006) and *myo-3*::GFP (Fares
349 and Greenwald, 2001). *vit-2* is vitellogenin produced and secreted from intestinal cells
350 and taken up by the germline (Grant and Hirsh, 1999). *myo-3*::ssGFP has a signal
351 sequence on the fluorophore and is expressed in body wall muscle (Fares and

352 Greenwald, 2001) Two published studies examine genome-wide mRNA expression
353 patterns when *vit-2* is overexpressed or misregulated. First, we used WormCat to
354 examine category enrichment data from germline-less *glp-1* mutants obtained by the
355 Blackwell lab, where they showed that *vit-2*::GFP builds up near its production site in
356 the intestines (Steinbaugh et al., 2015)and found strong enrichment patterns in
357 STRESS RESPONSE: Pathogen: other (Fig5A). Next, we used WormCat to examine
358 RNA-seq data from VIT-2::GFP (Singh and Aballay, 2017) overexpressing animals
359 produced by the Aballay group and also fund increased stress response genes (**Fig5B).**
360
361 In order to more directly test the hypothesis that increased protein load could lead to
362 activation of these ILGs, we compared two strains with a differing copy number of *vit-2*;
363 RT130, made by microparticle bombardment and containing the GFP array in addition
364 to wild type copies (Balklava et al., 2016) and BCN9071 which is a CRISPR-generated
365 allele integrated into the endogenous locus (Rompay et al., 2015) (**Fig4E**). Van
366 Rompay reported that total yolk protein levels were higher in strains harboring *vit-*
367 *2*::GFP derived from RT130 (Rompay et al., 2015). Where we found by RT-PCR that
368 GFP expression levels were also increased (**Fig4F**). Thus, increasing the amount of
369 VIT-2::GFP produced was also associated with ILG upregulation.
370
371 We found that ILGs become upregulated in the absence of pathogen response when
372 lipid levels become unbalanced, ARF-1 functions are compromised, or when protein
373 production is increased. We next tested whether increased ILG expression was part of
374 a response to help stimulate passage through the secretory pathway when trafficking

375 load is high. One of the most strongly upregulated genes is *hpo-6*, which is not present
376 in any of the commercially available RNAi libraries. To study its function more closely in
377 this context, we made a cDNA construct to allow RNAi in VIT-2::GFP RT130 in wild type
378 and *sams-1(lof)* animals (Ding et al., 2015). *hpo-6* was originally identified in a screen
379 for genes whose loss increased sensitivity to a pore-forming toxin (Kao et al., 2011). It
380 has a glycoprotein domain and may occur in membrane rafts (Rao et al., 2011), but has
381 no apparent homology to human proteins . *hpo-6(RNAi)* causes a slight increase in
382 VIT-2::GFP in wild-type animals (**Fig6S**). However, in the low PC *sams-1(lof)*
383 background, VIT-2::GFP pooling and aggregation suggested a broad effect on
384 trafficking patterns (**Fig6S)**. Yolk in *C. elegans* consists of both lipids and proteins
385 (Perez and Lehner, 2019). Because low lipid levels in *sbp-1(RNAi)* animals makes
386 results with VIT-2::GFP difficult to interpret, we used the *myo-3*::ssGFP reporter model
387 (Fares and Greenwald, 2001), which expresses and secretes GFP in body wall muscle
388 cells. We used this reporter to examine the effects of *hpo-6* on secretion when *sbp-1*
389 function is reduced. First, we confirmed that knockdown of *arf-1* or *sbp-1* affected
390 secretion of the reporter, finding broad pooling and aggregation after *arf-1(RNAi)* and
391 aggregation with *sbp-1(RNAi)* (**Fig5H**). As in VIT-2::GFP, *hpo-6(RNAi)* had modest
392 effects in the wild-type background, with the appearance of small aggregates. (**Fig5H**).
393 In order to test the effects of blunting *hpo-6* upregulation in sbp-1 animals, we crossed
394 *myo-3*::ssGFP into a strain harboring a hypomorphic *sbp-1* allele *sbp-1(ep79)* (Brock et
395 al., 2006). We found that *hpo-6* knockdown increased the pooling and aggregation in
396 *myo-3::ssGFP*; *sbp-1(ep79)* animals (**Fig5I**). This suggests that some of ILGs respond

397 to changes in secretory function that could occur with lipid imbalance, trafficking load, or

398 pathogen exposure and support secretory function.

399

400

401 ## Discussion

402 Cellular stress arises when essential functions are limited or become unbalanced.
403 Membranous organelles are sensitive to both changes in intrinsic protein activity or
404 alterations of lipids within their bilayers and elicit gene expression programs when
405 stressed. While some stress-responsive genes have clear functions, many genes are
406 defined solely as being responsive to specific stresses (Holdorf et al., 2019; Nadal et al.,
407 2011). It is striking that altering membrane lipids activates a gene expression program
408 shared with pathogen stress in both *C. elegans* (Ding et al., 2015; Ho et al., 2020; Jung
409 et al., 2020) and mammals (Wu and Näär, 2019). Mammalian SREBP-1a has also
410 been implicated as a regulator of innate immune gene expression in macrophages (Im
411 et al., 2011). The secretory pathway is relevant to both membrane stress and immune
412 function about might therefore be regulated by both responses. Membrane organelles
413 such as the ER and Golgi are part of a more extensive trafficking system where proteins
414 and lipids are created, modified, then sent to proper intercellular locations or secreted
415 (Yarwood et al., 2020). Innate immune responses challenge trafficking systems as
416 antimicrobial peptides are produced in mass in the ER, sent in lipid vesicles to the
417 Golgi, where many are glycosylated and then packaged into lipid vesicles for secretion
418 (Bednarska et al., 2017). For example, the *C. elegans* genome contains more than 300
419 genes that are produced in response to specific pathogens (Engelmann et al., 2011)
420 and share similarity to known antimicrobial effectors (Dierking et al., 2016). In addition,
421 pathogen-responses require an intact ER stress pathway to allow adjustment to the
422 increased trafficking load (Lamitina and Chevet, 2012; Richardson et al., 2010).
423

424 The ER contains multiple pathways that respond to changes in proteostasis and lipid
425 levels (Gardner et al., 2013). These processes are orchestrated by ER-intrinsic proteins
426 that sense changes in protein folding or alterations in the lipid bilayer and have
427 important roles in basal conditions, as well as when the secretory system is overloaded
428 (Hotamisligil and Davis, 2016; Safra et al., 2013). ER-linked events are also important
429 during pathogen exposure in *C. elegans*; changes in ribosomal function at the ER have
430 a well-defined impact on pathogen responses (Dunbar et al., 2012; McEwan et al.,
431 2012) and pathogen responses depend on ER stress pathways (Richardson et al.,
432 2010; Tillman et al., 2018). Interestingly, the Lee lab also found that ILGs are
433 upregulated when trafficking is inhibited through blocking glycosylation in the ER (Jeong
434 et al., 2020). Other organelles in the secretory pathway, such as the Golgi, have their
435 own stress sensors and response pathways (Machamer, 2015). Our results suggest
436 that disruption of trafficking outside the ER by targeting ARF-1 in the Golgi can also
437 initiate a stress response stimulating ILG induction.
438
439 Genes upregulated by pathogen exposure include both antimicrobial effectors and
440 many genes of unknown function (Estes et al., 2010; Troemel et al., 2006). Notably, the
441 ILGs enriched after membrane stress are primarily those of unknown function. Several
442 lines of evidence prompted us to hypothesize that some of these genes might be part of
443 a response linked to stress in membranes of the secretory pathway rather than a direct
444 response to an extrinsic pathogen. First, the involvement of secretory organs was
445 implicated by alterations in PC ratios in the ER/Golgi in both *sams-1* and *sbp-1* RNAi
446 lipidomes. Second, our targeted RNAi screen for regulators of p*sysm-1::GFP* identified

447 the *arf-1* GTPase and coatomer proteins, which are critical Golgi/ER transport.
448 Importantly, knockdown of *arf-1* was sufficient to induce ILG upregulation.
449 Strengthening this link between disruption of lipid levels and ARF-1 function, we also
450 found *sbp-1* RNAi altered ARF-1::RFP localization and Golgi morphology.
451
452 ARF-1 is a critical regulator of trafficking, coordinating retrograde traffic from the Golgi
453 to the ER and regulating secretory function in the trans-Golgi (Donaldson and Jackson,
454 2011). Cycling of ARF-1 GTPases depends on membrane localization of the ARF
455 GTPase, GEF, and GAP (GTPase activating protein) (Donaldson and Jackson, 2011).
456 We previously found that knockdown of PC synthesis enzymes blocked ARF1 cycling
457 and limited membrane association of the ARF GEF GBF1 in cultured human cells
458 (Smulan et al., 2016). This suggests low PC levels affect ARF1 activity by limiting the
459 ability of the GTPase, GEF, and GAP to associate at the Golgi membrane and initiate
460 GDP-GTP cycling. However, PC could be linked to ARF1 through other mechanisms.
461 ARF1 and phospholipase D (PLD) function have been linked by multiple labs (Riebeling
462 et al., 2009). PLD cleaves PC molecules to produce choline and phosphatidic acid,
463 which in turn stimulates vesicle formation (McDermott et al., 2004). This regulatory loop
464 requires PC, which is low in ER/Golgi membranes in *sams-1* and *sbp-1* RNAi animals.
465 DAG kinases, which could be stimulated by changes in DAGs in the *sbp-1* or *sams-*
466 *1(RNAi)* animals, can also affect ARF activity and trafficking (Huijbregts et al., 2000).
467 Finally, Protein Kinase D has an important role in maintaining Golgi structure, and its
468 ortholog has been linked to immunity in *C. elegans* (Malhotra and Campelo, 2011; Ren
469 et al., 2009). However, none of these components activated the p*sysm-1::GFP* reporter

470 in our RNAi screen, suggesting they could be important in other regulatory contexts.
471 Indeed, the breadth of change in the lipidomes after *sams-1* or *sbp-1* RNAi suggests
472 that other inputs could link lipids and ILG expression. In addition, other cellular
473 processes may also affect ILG expression either in basal conditions or during pathogen
474 infection. For example, there is a complex relationship between pathogen infection,
475 proteotoxic stress, and induction of ILGs (Reddy et al., 2017)
476
477 In conclusion, our data suggest that the ILG induction after both broad disruption in
478 membrane lipids and pathogen exposure occurs because both processes stress the
479 trafficking system. We also find that one the upregulated immune-linked genes, *hpo-6*,
480 can facilitate trafficking function. Our results suggest ILG induction may represent a
481 "multi-membrane" stress response encompassing the roles of both the ER and the
482 Golgi in trafficking. Many mammalian studies on the effect of lipids on innate immune
483 functions have focused on specific lipids as stimulators of signaling pathways (Barnett
484 and Kagan, 2019). Taken together, these results suggest that levels of specific
485 membrane lipids can initiate stress responses sensitive to trafficking defects, which
486 could impact immune function as well as other secretion-dependent processes. Cells
487 contain complex systems for managing stress in the initial organelle of the secretory
488 process, the ER, which may respond to disturbances in protein synthesis, aggregation,
489 or lipid imbalances with specific programs of gene expression (Costa-Mattioli and
490 Walter, 2020; Hotamisligil and Davis, 2016). Thus, the expression of ILGs may reflect a
491 broader stress response that affects multiple secretory organelles, as processes beyond
492 translation and folding are affected.

493 ## Experimental Model and Subject Details

494 ***C. elegans* strains, RNAi constructs, and screening**.

495 N2 (wild type), p*sysm-1::GFP,* and OP50 were obtained from the *Caenorhabditis*
496 Genetics Center. CRISPR-tagged ARF-1, p*arf-1::arf-1::RFP,* was obtained from *In vivo*
497 Biosystems and outcrossed 3 times. Normal growth media (NGM) was used unless
498 otherwise noted. For RNAi, gravid adults were bleached onto NGM plates
499 supplemented with ampicillin, tetracycline, and 6mM IPTG and 10X concentrated
500 bacterial cultures. *C. elegans* were allowed to develop until the young adult stage
501 before harvesting. Because of larval arrest, *copa-1* RNAi bacteria were diluted 1:10 in
502 control RNAi bacteria before plating. For the RNAi screen, L1 larvae were plated into
503 96 well plates spotted with RNAi bacteria, and L4/young adults were scored from -3 to
504 +3 with 0 as no change in 4 independent replicates.

505

506 **Cell culture and siRNA transfection**

507 HepG2 cells (ATCC, HB-8065) were grown in Minimum Essential Medium (Invitrogen)
508 plus 10% FBS (Invitrogen), Glutamine (Invitrogen), and Sodium Pyruvate (Invitrogen).
509 siRNA oligonucleotides transfections were done for 48 hours using Lipofectamine
510 RNAiMAX Transfection Reagent (Invitrogen, 13778100), and cells were held for 16
511 hours in 1% Lipoprotein Deficient Serum (LDS) (Biomedical Technologies, BT907) and
512 25 µg/ml ALLN (Calbiochem) for 30 min prior to harvesting.

513

514 **Immunoblotting:**

515 **HepG2 cells:** Syringe passage was used to lyse cells in High Salt RIPA (50 mM Tris,
516 pH 7.4; 400 mM NaCl; 0.1% SDS; 0.5% NaDeoxycholate; 1% NP-40; 1 mM DTT, 2.5
517 µg/mL ALLN, Complete protease inhibitors (Roche). Invitrogen NuPage gels (4- 12%)
518 were used for protein separation before transfer to nitrocellulose. Blots were probed
519 with antibodies to phosphorylated p38 MAP Kinase, total p38, and STAT1 were used as
520 a control. Immune complexes were visualized with Luminol Reagent (Millipore).
521 Densitometry was performed by scanning the film, then analysis of pixel intensity with
522 ImageJ software. Graphs show the average of at least three independent experiments
523 with control values normalized to one.
524
525 ***C. elegans:*** Young adult animals were lysed by sonication in High Salt RIPA, and
526 immunoblotting was performed as above.
527
528 **Microscopy**
529 P*sysm*-1::GFP *C. elegans* strains were grown until the L4/young adult transition, and
530 images were acquired on a Zeiss Dissecting Scope with an Axiocam camera. ARF-
531 1::RFP and MANS-1::GFP images were acquired on a Leica SPE confocal, and
532 projections of confocal slices were produced. All images were taken at identical gain
533 settings within experimental sets, and Adobe Photoshop was used for corrections to
534 levels across experimental sets.
535
536 **Lipidomics**

537 *C. elegans* total and microsomal lipidomics, including fractionation protocols, were
538 performed at the Whitehead Metabolomics core as in Smulan et al. 2016. Statistical
539 analysis was performed in Graphpad prism.
540
541 **Gene expression analysis**
542 Lysis of young adult *C. elegans* was performed in 0.5% SDS, 5% β-ME, 10 mM EDTA,
543 10 mM Tris-HCl ph7.4, 0.5 mg/ml Proteinase K, before purification of RNA by TRI-
544 Reagent (Sigma). cDNA was produced with Transcriptor First-strand cDNA kits
545 (Roche), and RT-PCR was performed using Kappa SYBR Green 2X Mastermix.
546
547 RNA for sequencing was purified using RNAeasy columns (Qiagen). RNA sequencing
548 (including library construction was performed by BGI (Hong Kong). Reads were
549 analyzed through the Dolphin analysis platform (https://dolphin.umassmed.edu/), using
550 DeSeq to identify differentially expressed genes (Yukselen et al., 2020). Gene set
551 enrichment was performed using WormCat (www.wormcat.com) (Holdorf et al., 2019).
552
553

Acknowledgments

We would like acknowledge Drs. Seung-Jae Lee, Sujeong Kwon (Korea Advanced Institute of Science and Technology) for providing the *lpin-1* RNA seq data. We would also like to thank Drs. Seung-Jae Lee, Emily Troemel (USD) and members of the Walker lab for comments on the manuscript as well as Dr. Marian Walhout (UMASS Chan School of Medicine) for helpful discussion. We would like to acknowledge Wei Ding for technical support and Caroline Lewis (MIT) for metabolomics screening at the Whitehead Metabolomics core. We also thank Life Science Editors and Dr. Sabbi Lall for manuscript editing. Funding was from the NIA at the NIH: R01AG053355 and R56AG068670. Some strains were provided by the CGC, which is funded by the NIH Office of Research Infrastructure Programs (P40 OD010440).

Author Contributions

Conceptualization; AKW, CMW, LJS

Verification: AKW, CMW, LJS

Formal Analysis: AKW, CMW, LJS

Investigation: AKW, CMW, LJS, DL, MF

Resources: AKW

Data Curation: AKW

Writing: AKW

Writing/Editing: AKW, CMW, LJS,

Visualization: AKW

Supervision: AKW

Funding: AKW

Declaration of Interests

The authors declare no competing interests

594 ## Figure Legends

595 **Figure 1: Upregulation of immunity-linked genes occurs downstream of multiple**
596 **types of membrane lipid disruption.** WormCat gene set enrichment shows STRESS
597 RESPONSE (**A**) and STRESS RESPONSE: Pathogen (**B**) are upregulated in *lpin-1*
598 RNAi animals, as in *sams-1* and *sbp-1(RNAi)* animals (Ding et al., 2015). Legend is in
599 **C**. qRT-PCR shows that upregulation of an immunity-linked gene, *hpo-6*, in *sams-1(lof)*
600 animals is not dependent on *sbp-1* (**D**).
601
602 **Figure 2: Broad lipidomic changes in total and microsomal lipid compartments**
603 **after *sams-1* or *sbp-1* RNAi**. LC/MS lipidomics show that nearly a third of total lipid
604 species change after *sams-1* or *sbp-1* RNAi (**A, B**). Significant changes in major lipid
605 classes are mostly distinct in *sams-1* and *sbp-1* RNAi (**C, D**). See also **Figure S1** (**B,**
606 **D**) for lipid species distributions and additional lipid class analysis. The microsomal
607 (ER/Golgi) lipidome is also broadly altered after *sbp-1 RNAi* (**E**) and shows changes in
608 different lipid classes than in the total lipidome (**F, G**). Error bars show standard
609 deviation. Lipid class data is calculated by students T-Test. See Figure S1 for lipid
610 species distributions and additional lipid class analysis.
611
612 **Figure 3: Targeted RNAi screen reveals candidates linked to Golgi/ER trafficking**
613 **and ceramide/sphingomyelin synthesis impact immunity gene expression.** (**A**)
614 Immune gene reporter p*sysm-1*::GFP is increased after *sbp-1* RNAi. (**B**) Screen
615 schematic. (**C**) Schematic showing RNAi library coverage and screen candidates.
616 Epifluorescence imaging showing validation of reporter activity after RNAi of lipid PC

617 synthesis genes (**D**), SM synthesis genes (**E**) and the SCD *fat-7* (**F**). Epifluorescence
618 images showing GFP levels after RNAi of the *arf-1* GTPase or coatomer component
619 *copa-1* (**I**). Because of poor larval development, bacterial for *copa-1* RNAi was diluted
620 to 1:10. **J**. Epifluorescence images showing GFP levels genes linked to Golgi function.
621 For qRT-PCR, see **Figure S4.**
622
623 **Figure 4: Disruption of Golgi/ER trafficking increases expression of immunity-**
624 **related genes. A.** Scatter plot shows changes in gene expression after *arf-1* RNAi. **B.**
625 WormCat gene set enrichment chart shows an increase in stress response and
626 pathogen linked genes. **C.** Confocal projections of CRISPR tagged ARF-1::RFP reveal
627 that that Golgi-specific pattern is disrupted after *sbp-1* RNAi. Scale bar is 10 microns.
628 **D**. Confocal projections of the *C. elegans* Golgi marker MANS::GFP (Chen et al., 2006)
629 in Control, *sbp-1, arf-1,* and *copa-1 (1:10)* RNAi intestines. Scale bar is 10 microns.
630
631 **Figure 5: Immunity-linked genes are linked to trafficking disruption.** WormCat
632 gene enrichment of upregulated genes from *glp-1*(AA2735) (Steinbaugh et al., 2015)
633 and *vit-2(ac3)* compared to SJ4005 (Singh and Aballay, 2017)for Category 1 (**A**) and
634 Category 2 (**B**). Legend is in **C**. qRT-PCR comparing gene expression in wild type,
635 single copy *vit-2::GFP* (BCN9071, s) or multi copy (RT130, m) animals. **D** and **E** show
636 increase in GFP or *vit-2*. Immune response genes are shown in **F-I**. **J.** Confocal
637 images of body wall muscle cells expressing of the secretion marker *myo-3*::ssGFP. **K**.
638 Body wall muscle cells in imaged by confocal microscopy in *myo-3*::ssGFP; *sbp-1(ep79)*
639 animals.

640 ## Supplemental information

641 **Figure S1: Activation of Stress response pathways when PC synthesis is**
642 **disrupted. A.** WormCat analysis of microarray data from Koh, et al. 2018. **B.** The p38
643 MAP kinase MAPK14 is phosphorylated after siRNA of *PCYT1* in human hepatoma
644 cells. **C.** Constitutive phosphorylation of the *C. elegans* MAPK14 ortholog, PMK-1,
645 occurs after both *sams-1* and *sbp-1(RNAi)*.
646
647 **Figure S2: Broad lipidomic changes in total and microsomal lipid compartments**
648 **after *sams-1* or *sbp-1* RNAi**. **A**. Schematic showing effects of PC producing pathways
649 on ARF-1. Tables showing numbers lipid species within each class in the total lipidome
650 (**B**) or ER/Golgi lipidome in *sbp-1(RNAi)* animals (**D**). Green boxes denote classes in
651 which the distribution of the species within each RNAi significantly differed from controls
652 using the Wilcoxen test for non-parametric data. Levels of lipid classes in total *sams-1*
653 or *sbp-1* total lipidomics (**C**) or *sbp-1* ER/Golgi lipidomics (**E**).
654
655 **Figure S3: Candidates from lipid sub-library RNAi screen.** Table showing
656 candidates from quadruplicate screening of the RNAi sub-library along with other genes
657 selected as controls for the rescreen.
658
659 **Figure S4: Regulation of immunity-linked genes in conditions of membrane**
660 **disruption.** qRT PCR quantitating GFP upregulation after knockdown of Golgi
661 trafficking regulators **(A)** or lipid synthesis genes **(B)**. qRT-PCR from *psysm-1*::GFP (A-

662 H) or p*sysm-1*::GFP; *sbp-1(ep79)* (I-K) shows effects of disrupting *arf-1* or membrane
663 lipids on ILGs. Error bars show standard deviation.
664
665 **Figure S5: Shared upregulation of immunity linked genes in *sams-1, sbp-1* and**
666 ***arf-1* transcriptomic studies.** Venn diagrams showing limited overlap of up- (A) or
667 downregulated (**B**) genes after *sbp-1, sams-1* or *arf-1* RNAi. **C-D.** WormCat analysis
668 comparing overlapping gene sets from *arf-1, sbp-1* and *sams-1* upregulated genes.
669 Data for *arf-1* alone is the same as **Figure 4B**. Legend is in **E**. Confocal micrographs
670 showing minimal changes after *sptl-1* RNAi in of MANS::GFP (**F**) or ARF-1::RFP (**G**).
671 Bar show 10 microns.
672
673 **Figure S6: Reduction in *hpo-6* exacerbates *sams-1(lof)* trafficking defects.**
674 Confocal projections of *C. elegans* intestinal cells expressing *vit-2*::GFP (RT130) in wild
675 type or *sams-1(lof)* backgrounds.
676
677 **Table S1: Transcriptomics and gene set enrichment from *lpin-1(RNAi)* animals.** 2
678 fold upregulated genes in *lpin-1(RNAi)* animals. Gene set enrichment was performed
679 using WormCat (Holdorf et al., 2019).
680
681 **Table S2**: **Total lipidomics of *sams-1* and *sbp-1(RNAi)* animals and microsomal**
682 **lipidomics of *sbp-1(RNAi)* adults.** Datasets from two lipidomic studies. The first is
683 LCMS data normalized to total lipids compared between Control, *sbp-1,* and *sams-*
684 *1*(*RNAi)* adults. Tabs are labeled sams_sbp_Lipid class. The second dataset contains

685 LCMS from Control and *sbp-1(RNAi)* microsome preps from adult animals. Significance
686 of fold changes in individual lipids determined by students T-test.
687
688 **Table S3:** Results from the screen of the "lipid sub-library." Tabs 1 and 2 contain
689 averaged results from quadruplicate screening of *sysm-1*::GFP or *sysm-1::GFP; sbp-*
690 *1(ep79)*. The secondary screen contains averages from candidates selected from the
691 first screen, plus *fat-5, fat-6,* and *fat-7* as additional test RNAis. The secondary screen
692 was conducted in quadruplicate. ND is not done.
693
694 **Table S4**: Transcriptomic responses to trafficking disruption. RNAseq from control vs.
695 *arf-1/arf-1.2(RNAi)* animals (arf_1_all, arf_2Xup) and gene set enrichment analysis
696 produced in WormCat for Category 1, Category2 and Category3). WormCat analysis of
697 *vit-2*::GFP (Singh and Aballay, 2017)and *glp-1* (Steinbaugh et al., 2015) datasets.
698

699 **References**

700

701 Ackema, K.B., Sauder, U., Solinger, J.A., and Spang, A. (2013). The ArfGEF GBF-1 Is
702 Required for ER Structure, Secretion and Endocytic Transport in *C. elegans*. Plos One
703 *8*, e67076.

704 Aramburu, J., Ortells, M.C., Tejedor, S., Buxadé, M., and López-Rodríguez, C. (2014).
705 Transcriptional regulation of the stress response by mTOR. Sci Signal *7*, re2–re2.

706 Balklava, Z., Rathnakumar, N.D., Vashist, S., Schweinsberg, P.J., and Grant, B.D.
707 (2016). Linking Gene Expression in the Intestine to Production of Gametes Through the
708 Phosphate Transporter PITR-1 in *Caenorhabditis elegans*. Genetics *204*, 153 162.

709 Barnett, K.C., and Kagan, J.C. (2019). Lipids that directly regulate innate immune signal
710 transduction. Innate Immun *26*, 4–14.

711 Bednarska, N.G., Wren, B.W., and Willcocks, S.J. (2017). The importance of the
712 glycosylation of antimicrobial peptides: natural and synthetic approaches. Drug Discov
713 Today *22*, 919–926.

714 Bodhicharla, R., Devkota, R., Ruiz, M., and Pilon, M. (2018). Membrane Fluidity Is
715 Regulated Cell Non-autonomously by *Caenorhabditis elegans* PAQR-2 and Its
716 Mammalian Homolog AdipoR2. Genetics *210*, 189 201.

717 Boncompain, G., and Weigel, A.V. (2018). Transport and sorting in the Golgi complex:
718 multiple mechanisms sort diverse cargo. Curr Opin Cell Biol *50*, 94–101.

719 Brock, T.J., Browse, J., and Watts, J.L. (2006). Genetic Regulation of Unsaturated Fatty
720 Acid Composition in *C. elegans*. Plos Genet *2*, e108.

721 Broekhuis, J.R., Rademakers, S., Burghoorn, J., and Jansen, G. (2013). SQL-1,
722 homologue of the Golgi protein GMAP210, modulates intraflagellar transport in *C.*
723 *elegans*. J Cell Sci *126*, 1785–1795.

724 Chen, C.C.-H., Schweinsberg, P.J., Vashist, S., Mareiniss, D.P., Lambie, E.J., and
725 Grant, B.D. (2006). RAB-10 Is Required for Endocytic Recycling in the *Caenorhabditis*
726 *elegans* Intestine. Mol Biol Cell *17*, 1286 1297.

727 Costa-Mattioli, M., and Walter, P. (2020). The integrated stress response: From
728 mechanism to disease. Science *368*, eaat5314.

729 Couillault, C., Fourquet, P., Pophillat, M., and Ewbank, J.J. (2012). A UPR-independent
730 infection-specific role for a BiP/GRP78 protein in the control of antimicrobial peptide
731 expression in *C. elegans* epidermis. Virulence *3*, 299 308.

732 Dierking, K., Yang, W., and Schulenburg, H. (2016). Antimicrobial effectors in the
733 nematode *Caenorhabditis elegans*: an outgroup to the Arthropoda. Philosophical
734 Transactions Royal Soc B Biological Sci *371*, 20150299.

735 Ding, W., Smulan, L.J., Hou, N.S., Taubert, S., Watts, J.L., and Walker, A.K. (2015). s-
736 Adenosylmethionine Levels Govern Innate Immunity through Distinct Methylation-
737 Dependent Pathways. Cell Metab *22*, 633 645.

738 Donaldson, J.G., and Jackson, C.L. (2011). ARF family G proteins and their regulators:
739 roles in membrane transport, development and disease. Nat Rev Mol Cell Bio *12*, 362
740 375.

741 Dunbar, T.L., Yan, Z., Balla, K.M., Smelkinson, M.G., and Troemel, E.R. (2012). *C.*
742 *elegans* detects pathogen-induced translational inhibition to activate immune signaling.
743 Cell Host Microbe *11*, 375 386.

744 Engelmann, I., Griffon, A., Tichit, L., Montañana-Sanchis, F., Wang, G., Reinke, V.,
745 Waterston, R.H., Hillier, L.W., and Ewbank, J.J. (2011). A Comprehensive Analysis of
746 Gene Expression Changes Provoked by Bacterial and Fungal Infection in *C. elegans*.
747 Plos One *6*, e19055.

748 Estes, K.A., Dunbar, T.L., Powell, J.R., Ausubel, F.M., and Troemel, E.R. (2010). bZIP
749 transcription factor *zip-2* mediates an early response to Pseudomonas aeruginosa
750 infection in *Caenorhabditis elegans*. Proc National Acad Sci *107*, 2153 2158.

751 Fares, H., and Greenwald, I. (2001). Genetic Analysis of Endocytosis in *Caenorhabditis*
752 *elegans* : Coelomocyte Uptake Defective Mutants. Genetics *159*, 133–145.

753 Fletcher, M., Tillman, E.J., Butty, V.L., Levine, S.S., and Kim, D.H. (2019). Global
754 transcriptional regulation of innate immunity by ATF-7 in *C. elegans*. Plos Genet *15*,
755 e1007830.

756 Fraser, A.G., Kamath, R.S., Zipperlen, P., Martinez-Campos, M., Sohrmann, M., and
757 Ahringer, J. (2000). Functional genomic analysis of *C. elegans* chromosome I by
758 systematic RNA interference. Nature *408*, 325–330.

759 Gardner, B.M., Pincus, D., Gotthardt, K., Gallagher, C.M., and Walter, P. (2013).
760 Endoplasmic Reticulum Stress Sensing in the Unfolded Protein Response. Csh
761 Perspect Biol *5*, a013169.

762 Gianfrancesco, M.A., Paquot, N., Piette, J., and Legrand-Poels, S. (2018). Lipid bilayer
763 stress in obesity-linked inflammatory and metabolic disorders. Biochem Pharmacol *153*,
764 168–183.

765 Grant, B., and Hirsh, D. (1999). Receptor-mediated endocytosis in the *Caenorhabditis*
766 *elegans* oocyte. Mol Biol Cell *10*, 4311 4326.

767 Grant, B.D., and Sato, M. (2006). Intracellular trafficking. Wormbook Online Rev C
768 Elegans Biology 1–9.

769 Halbleib, K., Pesek, K., Covino, R., Hofbauer, H.F., Wunnicke, D., Hänelt, I., Hummer,
770 G., and Ernst, R. (2017). Activation of the Unfolded Protein Response by Lipid Bilayer
771 Stress. Mol Cell *67*, 673 684.e8.

772 Higgins, D.P., Weisman, C.M., Lui, D.S., D'Agostino, F.A., and Walker, A.K. (2021).
773 WormCat 2.0 defines characteristics and conservation of poorly annotated genes in
774 Caenorhabditis elegans. Biorxiv. https://doi.org/10.1101/2021.11.11.467968

775 Ho, N., Xu, C., and Thibault, G. (2018). From the unfolded protein response to
776 metabolic diseases – lipids under the spotlight. J Cell Sci *131*, jcs199307.

777 Ho, N., Yap, W.S., Xu, J., Wu, H., Koh, J.H., Goh, W.W.B., George, B., Chong, S.C.,
778 Taubert, S., and Thibault, G. (2020). Stress sensor Ire1 deploys a divergent
779 transcriptional program in response to lipid bilayer stress. J Cell Biol *219*.

780 Holdorf, A.D., Higgins, D.P., Hart, A.C., Boag, P.R., Pazour, G.J., Walhout, A.J.M., and
781 Walker, A.K. (2019). WormCat: An Online Tool for Annotation and Visualization of
782 *Caenorhabditis elegans* Genome-Scale Data. Genetics genetics.302919.2019.

783 HORTON, J.D., GOLDSTEIN, J.L., and BROWN, M.S. (2002). SREBPs: Transcriptional
784 Mediators of Lipid Homeostasis. Cold Spring Harb Sym *67*, 491–498.

785 Hotamisligil, G.S., and Davis, R.J. (2016). Cell Signaling and Stress Responses. Csh
786 Perspect Biol *8*, a006072.

787 Huijbregts, R.P.H., Topalof, L., and Bankaitis, V.A. (2000). Lipid Metabolism and
788 Regulation of Membrane Trafficking. Traffic *1*, 195–202.

789 Im, S.-S., Yousef, L., Blaschitz, C., Liu, J.Z., Edwards, R.A., Young, S.G., Raffatellu, M.,
790 and Osborne, T.F. (2011). Linking Lipid Metabolism to the Innate Immune Response in
791 Macrophages through Sterol Regulatory Element Binding Protein-1a. Cell Metab *13*,
792 540 549.

793 Jeong, D., Lee, D., Hwang, S., Lee, Y., Lee, J., Seo, M., Hwang, W., Seo, K., Hwang,
794 A.B., Artan, M., et al. (2017). Mitochondrial chaperone HSP-60 regulates anti-bacterial
795 immunity via p38 MAP kinase signaling. Embo J *36*, 1046–1065.

796 Jeong, D.-E., Lee, Y., Ham, S., Lee, D., Kwon, S., Park, H.-E.H., Hwang, S.-Y., Yoo, J.-
797 Y., Roh, T.-Y., and Lee, S.-J.V. (2020). Inhibition of the oligosaccharyl transferase in
798 *Caenorhabditis elegans* that compromises ER proteostasis suppresses p38-dependent
799 protection against pathogenic bacteria. Plos Genet *16*, e1008617.

800 Jung, Y., Kwon, S., Ham, S., Lee, D., Park, H.H., Yamaoka, Y., Jeong, D., Artan, M.,
801 Altintas, O., Park, S., et al. (2020). *Caenorhabditis elegans* Lipin 1 moderates the
802 lifespan-shortening effects of dietary glucose by maintaining ω-6 polyunsaturated fatty
803 acids. Aging Cell *19*.

804 Kao, C.-Y., Los, F.C.O., Huffman, D.L., Wachi, S., Kloft, N., Husmann, M., Karabrahimi,
805 V., Schwartz, J.-L., Bellier, A., Ha, C., et al. (2011). Global Functional Analyses of
806 Cellular Responses to Pore-Forming Toxins. Plos Pathog *7*, e1001314.

807 Klausner, R.D., Donaldson, J.G., and Lippincott-Schwartz, J. (1992). Brefeldin A:
808 insights into the control of membrane traffic and organelle structure. The Journal of Cell
809 Biology *116*, 1071 1080.

810 Koh, J.H., Wang, L., Beaudoin-Chabot, C., and Thibault, G. (2018). Lipid bilayer stress-
811 activated IRE-1 modulates autophagy during endoplasmic reticulum stress. J Cell Sci
812 *131*, jcs217992.

813 Lamitina, T., and Chevet, E. (2012). To UPR… and beyond!: A new role for a
814 BiP/GRP78 protein in the control of antimicrobial peptide expression in *C. elegans*
815 epidermis. Virulence *3*, 238–240.

816 Machamer, C.E. (2015). The Golgi complex in stress and death. Front Neurosci-Switz *9*,
817 421.

818 Malhotra, V., and Campelo, F. (2011). PKD Regulates Membrane Fission to Generate
819 TGN to Cell Surface Transport Carriers. Csh Perspect Biol *3*, a005280 a005280.

820 Mallo, G.V., Kurz, C.L., Couillault, C., Pujol, N., Granjeaud, S., Kohara, Y., and Ewbank,
821 J.J. (2002). Inducible Antibacterial Defense System in *C. elegans*. Curr Biol *12*, 1209–
822 1214.

823 McDermott, M., Wakelam, M.J.O., and Morris, A.J. (2004). Phospholipase D. Biochem
824 Cell Biol *82*, 225–253.

825 McEwan, D.L., Kirienko, N.V., and Ausubel, F.M. (2012). Host translational inhibition by
826 Pseudomonas aeruginosa Exotoxin A Triggers an immune response in *Caenorhabditis*
827 *elegans*. Cell Host Microbe *11*, 364 374.

828 McKay, R.M., McKay, J.P., Avery, L., and Graff, J.M. (2003). *C. elegans* A Model for
829 Exploring the Genetics of Fat Storage. Dev Cell *4*, 131–142.

830 Nadal, E. de, Ammerer, G., and Posas, F. (2011). Controlling gene expression in
831 response to stress. Nat Rev Genet *12*, 833–845.

832 Nhan, J.D., Turner, C.D., Anderson, S.M., Yen, C.-A., Dalton, H.M., Cheesman, H.K.,
833 Ruter, D.L., Naresh, N.U., Haynes, C.M., Soukas, A.A., et al. (2019). Redirection of

834 SKN-1 abates the negative metabolic outcomes of a perceived pathogen infection. Proc
835 National Acad Sci *116*, 22322–22330.

836 Pender, C.L., and Horvitz, H.R. (2018). Hypoxia-inducible factor cell non-autonomously
837 regulates *C. elegans* stress responses and behavior via a nuclear receptor. Elife *7*,
838 e36828.

839 Perez, M.F., and Lehner, B. (2019). Vitellogenins - Yolk Gene Function and Regulation
840 in *Caenorhabditis elegans*. Front Physiol *10*, 1067.

841 Radanović, T., Reinhard, J., Ballweg, S., Pesek, K., and Ernst, R. (2018). An Emerging
842 Group of Membrane Property Sensors Controls the Physical State of Organellar
843 Membranes to Maintain Their Identity. Bioessays *40*, 1700250.

844 Rao, W., Isaac, R.E., and Keen, J.N. (2011). An analysis of the *Caenorhabditis elegans*
845 lipid raft proteome using geLC-MS/MS. J Proteomics *74*, 242 253.

846 Reddy, K.C., Dror, T., Sowa, J.N., Panek, J., Chen, K., Lim, E.S., Wang, D., and
847 Troemel, E.R. (2017). An Intracellular Pathogen Response Pathway Promotes
848 Proteostasis in C. elegans. Curr Biol *27*.

849 Ren, M., Feng, H., Fu, Y., Land, M., and Rubin, C.S. (2009). Protein Kinase D Is an
850 Essential Regulator of C. elegans Innate Immunity. Immunity *30*, 521–532.

851 Richardson, C.E., Kooistra, T., and Kim, D.H. (2010). An essential role for XBP-1 in host
852 protection against immune activation in *C. elegans*. Nature *463*, 1092 1095.

853 Riebeling, C., Morris, A.J., and Shields, D. (2009). Phospholipase D in the Golgi
854 apparatus. Biochimica Et Biophysica Acta Bba - Mol Cell Biology Lipids *1791*, 876 880.

855 Rolls, M.M., Hall, D.H., Victor, M., Stelzer, E.H.K., and Rapoport, T.A. (2002). Targeting
856 of Rough Endoplasmic Reticulum Membrane Proteins and Ribosomes in Invertebrate
857 Neurons. Mol Biol Cell *13*, 1778–1791.

858 Rompay, L.V., Borghgraef, C., Beets, I., Caers, J., and Temmerman, L. (2015). New
859 genetic regulators question relevance of abundant yolk protein production in *C. elegans*.
860 Sci Rep-Uk *5*, 1 16.

861 Ruiz, M., Bodhicharla, R., Svensk, E., Devkota, R., Busayavalasa, K., Palmgren, H.,
862 Ståhlman, M., Boren, J., and Pilon, M. (2018). Membrane fluidity is regulated by the C.
863 elegans transmembrane protein FLD-1 and its human homologs TLCD1/2. Elife *7*,
864 1309.

865 Safra, M., Ben-Hamo, S., Kenyon, C., and Henis-Korenblit, S. (2013). The *ire-1* ER
866 stress-response pathway is required for normal secretory-protein metabolism in *C.*
867 *elegans*. J Cell Sci *126*, 4136–4146.

868 Sato, K., Sato, M., Audhya, A., Oegema, K., Schweinsberg, P., and Grant, B.D. (2006).
869 Dynamic Regulation of Caveolin-1 Trafficking in the Germ Line and Embryo of
870 *Caenorhabditis elegans*. Mol Biol Cell *17*, 3085 3094.

871 Shivers, R.P., Kooistra, T., Chu, S.W., Pagano, D.J., and Kim, D.H. (2009). Tissue-
872 Specific Activities of an Immune Signaling Module Regulate Physiological Responses to
873 Pathogenic and Nutritional Bacteria in *C. elegans*. Cell Host Microbe *6*, 321–330.

874 Singh, J., and Aballay, A. (2017). Endoplasmic Reticulum Stress Caused by Lipoprotein
875 Accumulation Suppresses Immunity against Bacterial Pathogens and Contributes to
876 Immunosenescence. Mbio *8*, e00778-17.

877 Smulan, L.J., Ding, W., Freinkman, E., Gujja, S., Edwards, Y.J.K., and Walker, A.K.
878 (2016). Cholesterol-Independent SREBP-1 Maturation Is Linked to ARF1 Inactivation.
879 Cell Reports *16*, 9 18.

880 Son, H.G., Altintas, O., Kim, E.J.E., Kwon, S., and Lee, S.V. (2019). Age-dependent
881 changes and biomarkers of aging in *Caenorhabditis elegans*. Aging Cell *18*, e12853.

882 Spang, A. (2002). ARF1 regulatory factors and COPI vesicle formation. Curr Opin Cell
883 Biol *14*, 423–427.

884 Steinbaugh, M.J., Narasimhan, S.D., Robida-Stubbs, S., Mazzeo, L.E.M., Dreyfuss,
885 J.M., Hourihan, J.M., Raghavan, P., Operaña, T.N., Esmaillie, R., and Blackwell, T.K.
886 (2015). Lipid-mediated regulation of SKN-1/Nrf in response to germ cell absence. Elife
887 *4*, 466.

888 Taguchi, T., and Mukai, K. (2019). Innate immunity signalling and membrane trafficking.
889 Curr Opin Cell Biol *59*, 1–7.

890 Tillman, E.J., Richardson, C.E., Cattie, D.J., Reddy, K.C., Lehrbach, N.J., Droste, R.,
891 Ruvkun, G., and Kim, D.H. (2018). Endoplasmic Reticulum Homeostasis Is Modulated
892 by the Forkhead Transcription Factor FKH-9 During Infection of *Caenorhabditis*
893 *elegans*. Genetics *210*, genetics.301450.2018.

894 Troemel, E.R., Chu, S.W., Reinke, V., Lee, S.S., Ausubel, F.M., and Kim, D.H. (2006).
895 p38 MAPK regulates expression of immune response genes and contributes to
896 longevity in *C. elegans*. Plos Genet *2*, e183.

897 Walker, A.K., Jacobs, R.L., Watts, J.L., Rottiers, V., Jiang, K., Finnegan, D.M., Shioda,
898 T., Hansen, M., Yang, F., Niebergall, L.J., et al. (2011). A Conserved SREBP-
899 1/Phosphatidylcholine Feedback Circuit Regulates Lipogenesis in Metazoans. Cell *147*,
900 840 852.

901 Watts, J.L., and Browse, J. (2002). Genetic dissection of polyunsaturated fatty acid
902 synthesis in *Caenorhabditis elegans*. Proc National Acad Sci *99*, 5854 5859.

903 Wellen, K.E., and Thompson, C.B. (2010). Cellular Metabolic Stress: Considering How
904 Cells Respond to Nutrient Excess. Mol Cell *40*, 323 332.

905 Wu, S., and Näär, A.M. (2019). SREBP1-dependent de novo fatty acid synthesis gene
906 expression is elevated in malignant melanoma and represents a cellular survival trait.
907 Sci Rep-Uk *9*, 10369.

908 Wu, Z., Isik, M., Moroz, N., Steinbaugh, M.J., Zhang, P., and Blackwell, T.K. (2019).
909 Dietary Restriction Extends Lifespan through Metabolic Regulation of Innate Immunity.
910 Cell Metab *29*, 1192-1205.e8.

911 Yang, F., Vought, B.W., Satterlee, J.S., Walker, A.K., Sun, Z.-Y.J., Watts, J.L.,
912 DeBeaumont, R., Saito, R.M., Hyberts, S.G., Yang, S., et al. (2006). An ARC/Mediator
913 subunit required for SREBP control of cholesterol and lipid homeostasis. Nature *442*,
914 700 704.

915 Yarwood, R., Hellicar, J., Woodman, P.G., and Lowe, M. (2020). Membrane trafficking
916 in health and disease. Dis Model Mech *13*, dmm043448.

917 Yukselen, O., Turkyilmaz, O., Ozturk, A.R., Garber, M., and Kucukural, A. (2020).
918 DolphinNext: a distributed data processing platform for high throughput genomics. Bmc
919 Genomics *21*, 310.

920 Zmora, N., Bashiardes, S., Levy, M., and Elinav, E. (2017). The Role of the Immune
921 System in Metabolic Health and Disease. Cell Metab *25*, 506–521.

922

Welsh, et al.
Figure 1

A

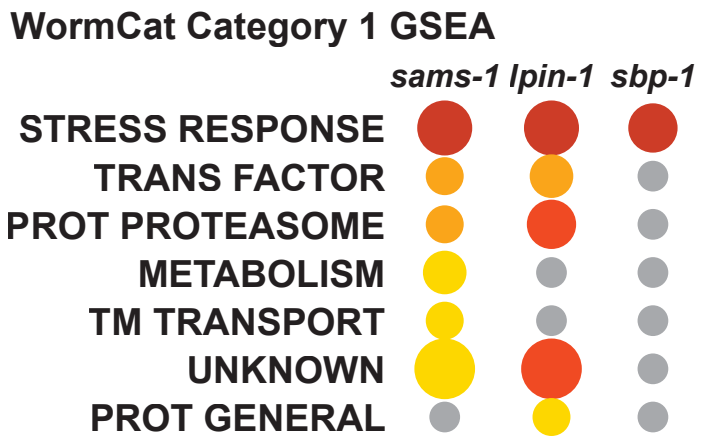

C

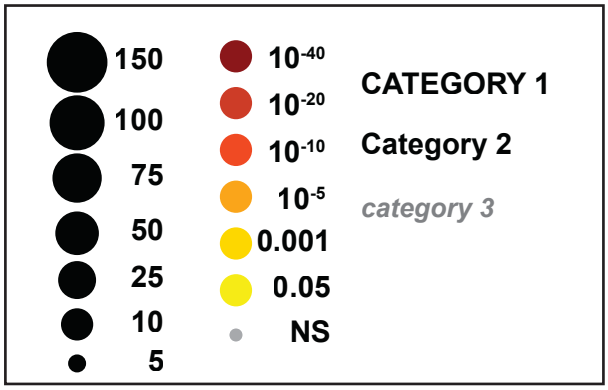

B

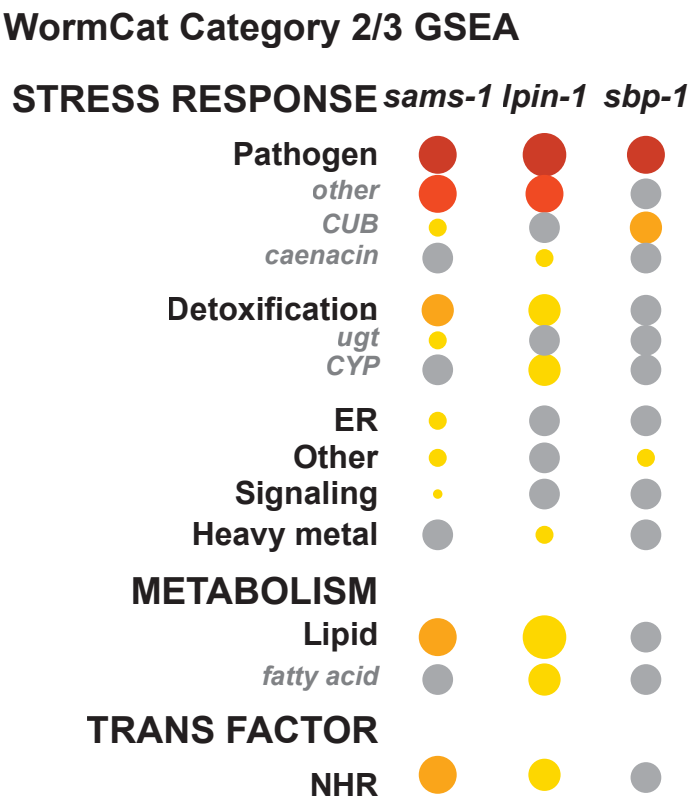

D

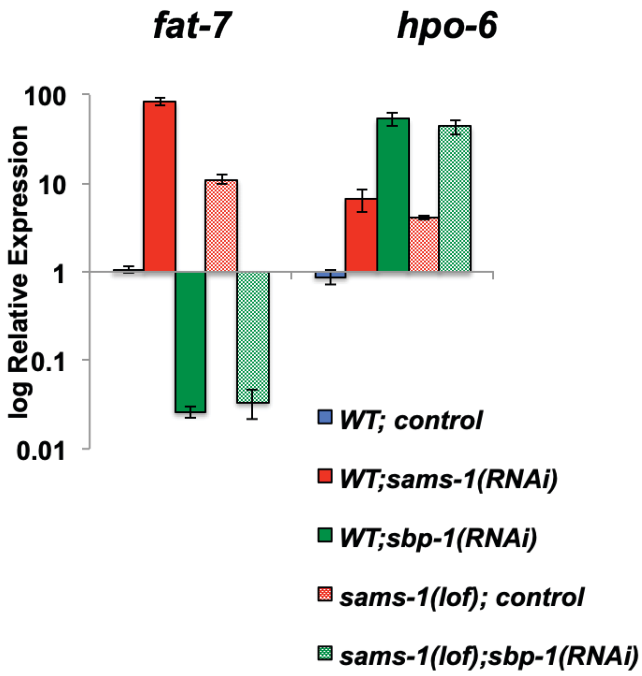

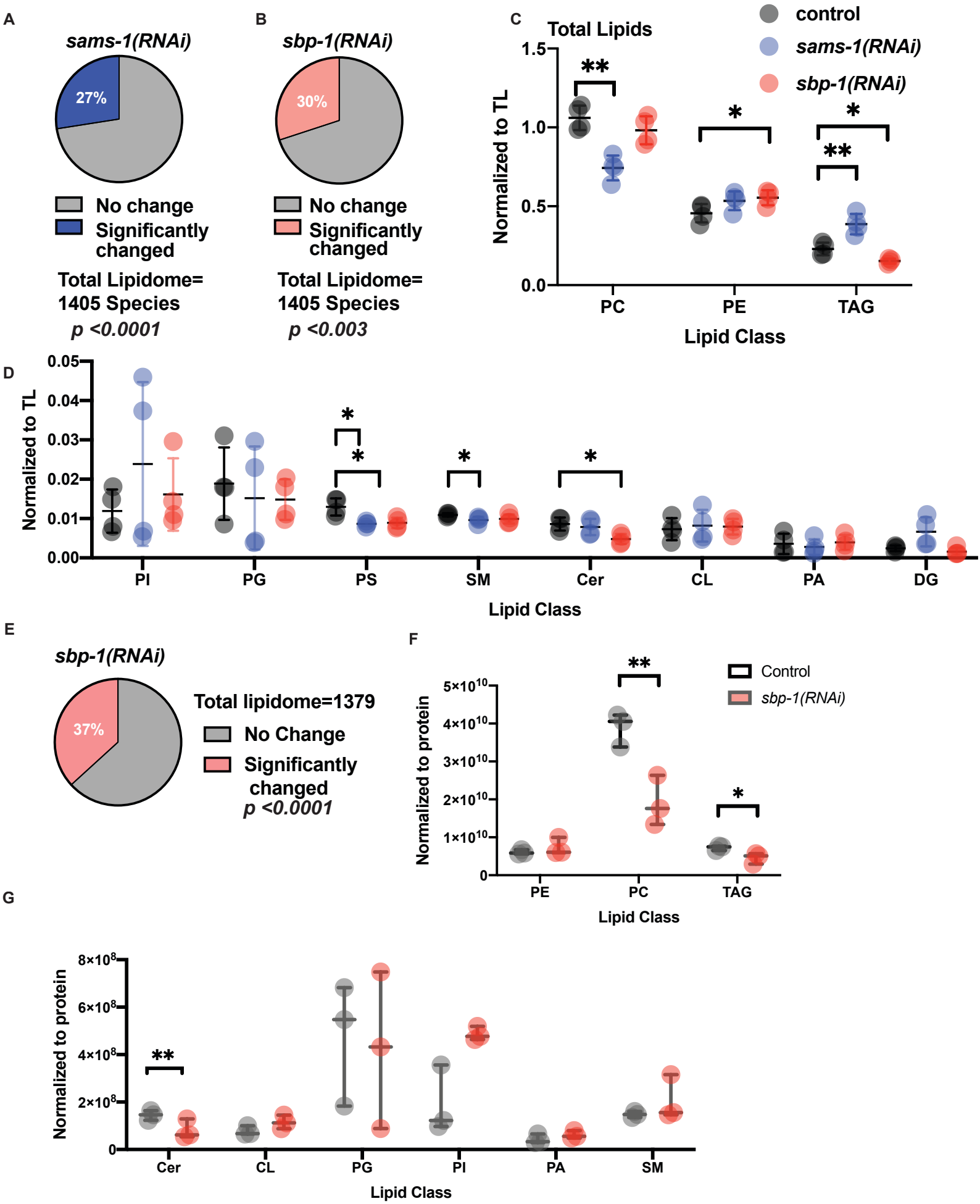
A
sams-1(RNAi)
27%
No change
Significantly changed
Total Lipidome= 1405 Species
p <0.0001
B
sbp-1(RNAi)
30%
No change
Significantly changed
Total Lipidome= 1405 Species
p <0.003
C
Total Lipids
control
sams-1(RNAi)
sbp-1(RNAi)
Normalized to TL
1.5
1.0
0.5
0.0
**
*
*
**
PC
PE
TAG
Lipid Class
D
Normalized to TL
0.05
0.04
0.03
0.02
0.01
0.00
*
*
*
*
PI
PG
PS
SM
Cer
CL
PA
DG
Lipid Class
E
sbp-1(RNAi)
37%
Total lipidome=1379
No Change
Significantly changed
p <0.0001
F
Control
sbp-1(RNAi)
Normalized to protein
5×10^10
4×10^10
3×10^10
2×10^10
1×10^10
0
**
*
PE
PC
TAG
Lipid Class
G
Normalized to protein
8×10^8
6×10^8
4×10^8
2×10^8
0
**
Cer
CL
PG
PI
PA
SM
Lipid Class

A

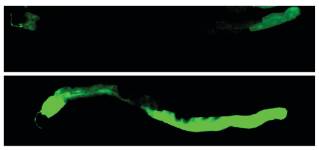
sysm-1::GFP
Control
sbp-1
(RNAi)

B

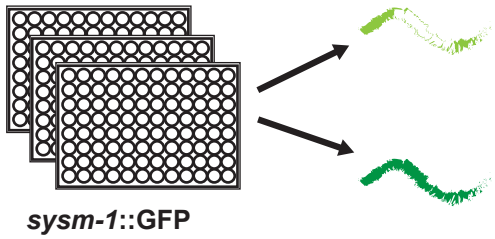
Complex Lipid
RNAi sublibrary 2.0
230 genes
sysm-1::GFP

C

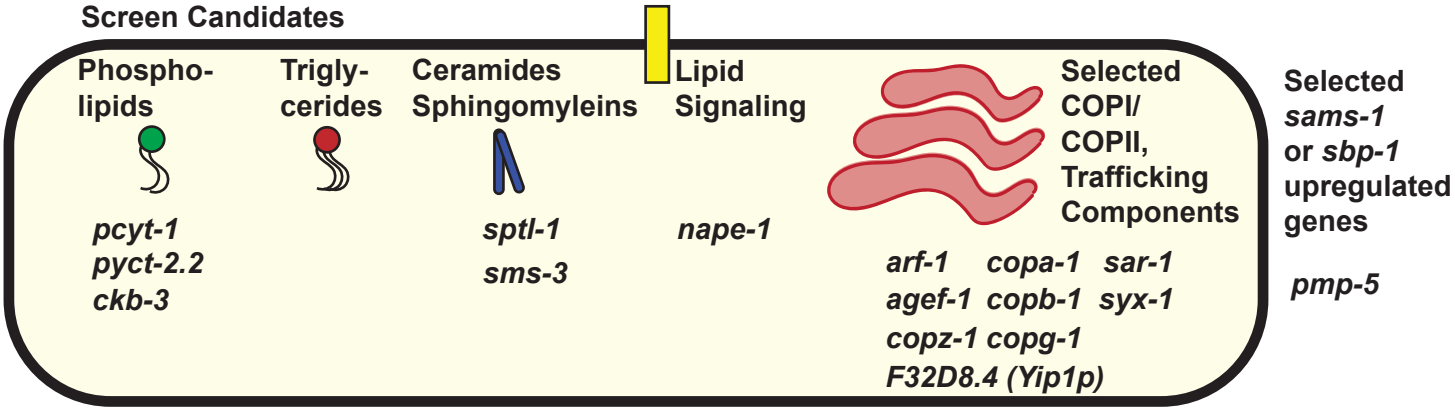
Screen Candidates
Phospho-
lipids
Trigly-
cerides
Ceramides
Sphingomyleins
Lipid
Signaling
Selected
COPI/
COPII,
Trafficking
Components
Selected
sams-1
or sbp-1
upregulated
genes
pcyt-1
pyct-2.2
ckb-3
sptl-1
sms-3
nape-1
arf-1 copa-1 sar-1
agef-1 copb-1 syx-1
copz-1 copg-1
F32D8.4 (Yip1p)
pmp-5

D

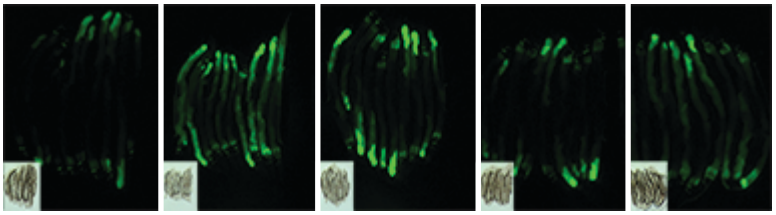
Control
sbp-1
pcyt-1
pcyt-2
pcyt-2.2
sysm-1::GFP

E

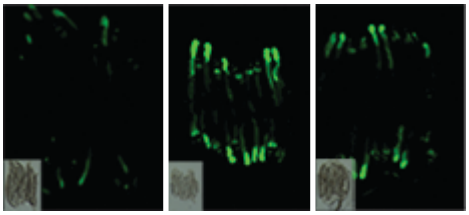
Control
sbp-1
ckb-3
sysm-1::GFP

F

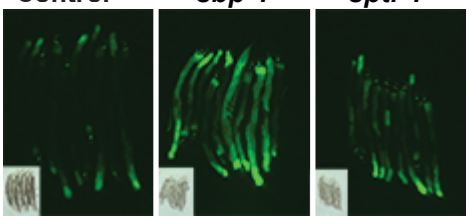
Control
sbp-1
sptl-1
sysm-1::GFP

G

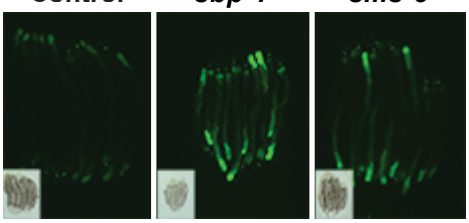
Control
sbp-1
sms-3
sysm-1::GFP

H

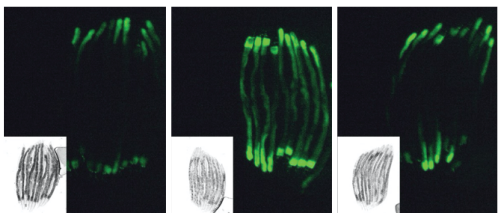
Control
sbp-1
fat-6
sysm-1::GFP

I

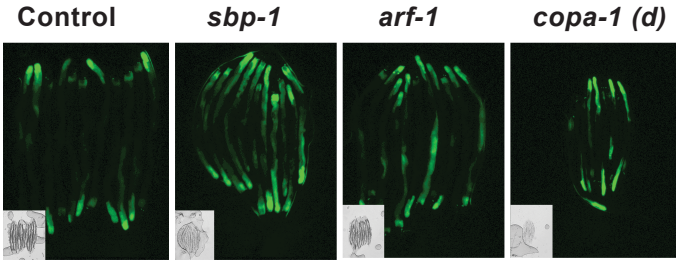
Control
sbp-1
arf-1
copa-1 (d)
sysm-1::GFP

J

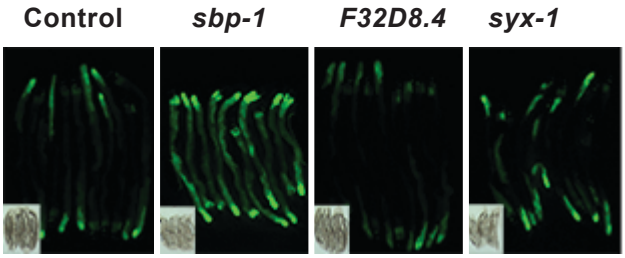
Control
sbp-1
F32D8.4
syx-1
sysm-1::GFP

A

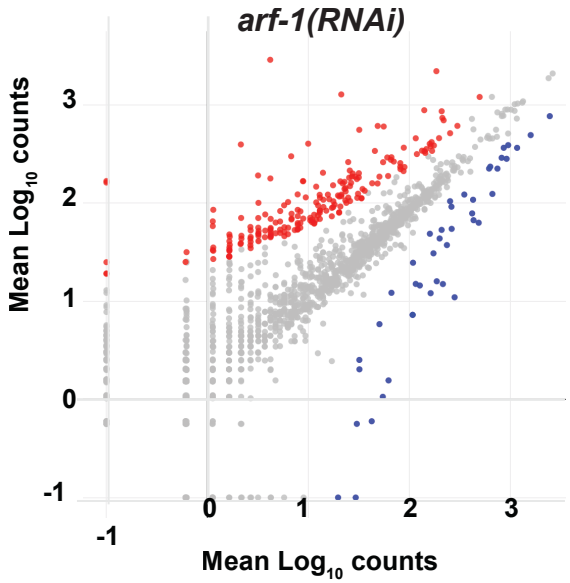
arf-1(RNAi)
Mean Log10 counts
Mean Log10 counts
3
2
1
0
-1
-1
0
1
2
3

B

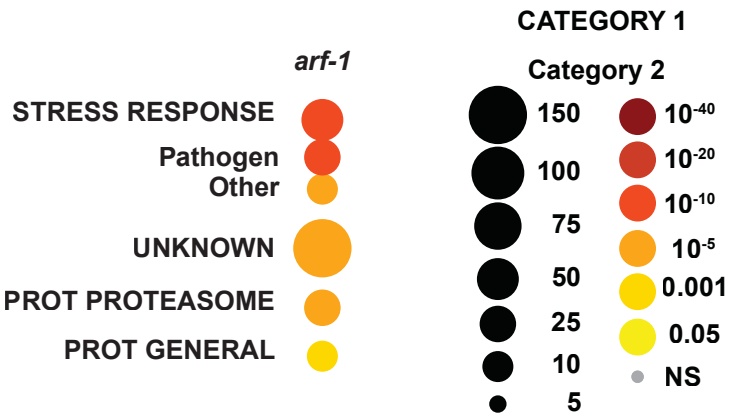
arf-1
STRESS RESPONSE
Pathogen
Other
UNKNOWN
PROT PROTEASOME
PROT GENERAL
CATEGORY 1
Category 2
150
100
75
50
25
10
5
10-40
10-20
10-10
10-5
0.001
0.05
NS

C

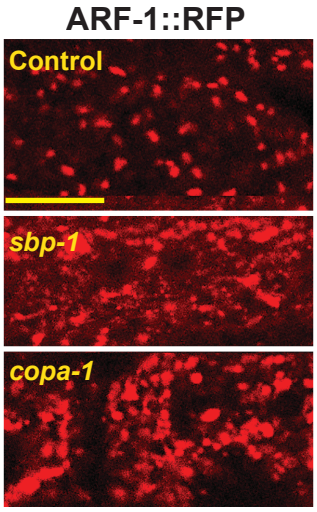
ARF-1::RFP
Control
sbp-1
copa-1

D

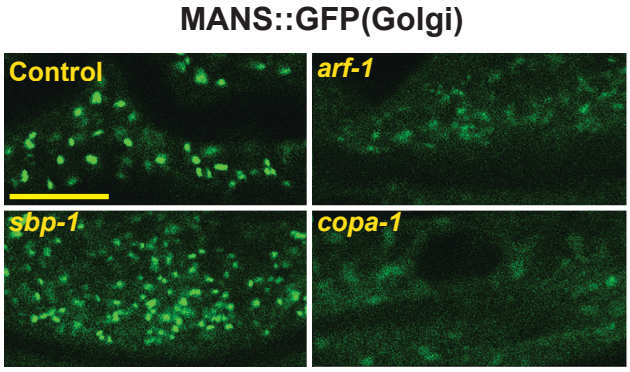
MANS::GFP(Golgi)
Control
arf-1
sbp-1
copa-1
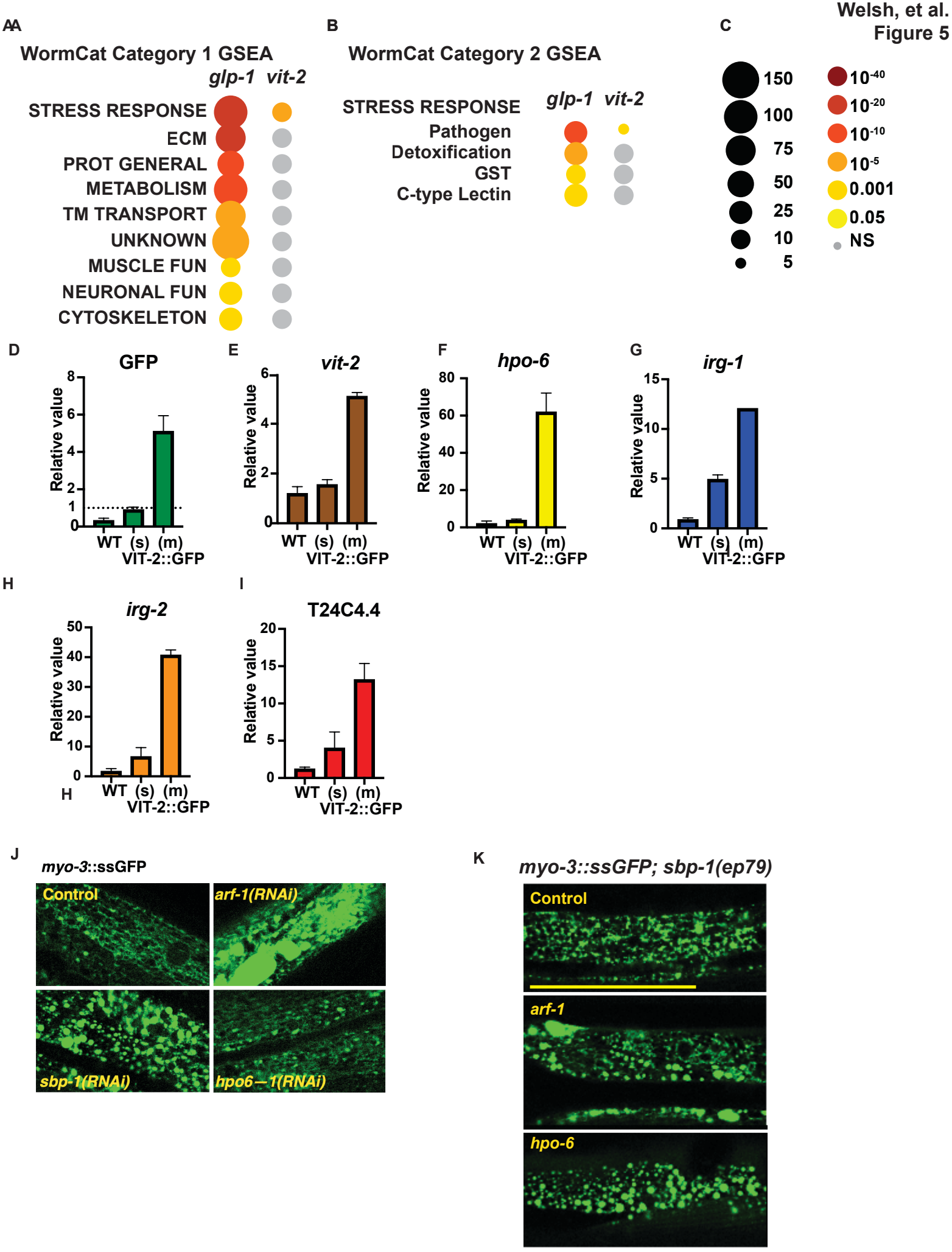
Welsh, et al.
Figure 5